International Journal of Pharmaceutics 409 (2011) 156–163

Contents lists available at ScienceDirect

International Journal of Pharmaceutics

journal homepage: www.elsevier.com/locate/ijpharm

Mechanistic models facilitate efficient development of leucine containing microparticles for pulmonary drug delivery

A.L. Feng[a], M.A. Boraey[a], M.A. Gwin[a], P.R. Finlay[a], P.J. Kuehl[b], R. Vehring[a,*]

[a] University of Alberta, Department of Mechanical Engineering, 4–9 Mechanical Engineering Building, Edmonton, Alberta, Canada T6G 2G8
[b] Lovelace Respiratory Research Institute, 2425 Ridgecrest Dr. SE, Albuquerque, NM 87108-5127, USA

ARTICLE INFO

Article history:
Received 21 December 2010
Received in revised form 28 January 2011
Accepted 21 February 2011
Available online 26 February 2011

Keywords:
Particle engineering
Spray drying
Respiratory drug delivery
Dispersibility
Powder density
Crystallinity

ABSTRACT

Mechanistic models of the spray drying and particle formation processes were used to conduct a formulation study with minimal use of material and time. A model microparticle vehicle suitable for respiratory delivery of biological pharmaceutical actives was designed. L-leucine was chosen as one of the excipients, because of its ability to enhance aerosol dispersibility. Trehalose was the second excipient. The spray drying process parameters used to manufacture the particles were calculated *a priori*. The kinetics of the particle formation process were assessed using a constant evaporation rate model. The experimental work was focused on the effect of increasing L-leucine mass fraction in the formulation, specifically its effect on leucine crystallinity in the microparticles, on powder density, and on powder dispersibility. Particle, powder and aerosol properties were assessed using analytical methods with minimal sample requirement, namely linear Raman spectroscopy, scanning electron microscopy, time-of-flight aerodynamic diameter measurements, and a new technique to determine compressed bulk density of the powder. The crystallinity of leucine in the microparticles was found to be correlated with a change in particle morphology, reduction in powder density, and improvement in dispersibility. It was demonstrated that the use of mechanistic models in combination with selected analytical techniques allows rapid formulation of microparticles for respiratory drug delivery using batch sizes of less than 80 mg.

1. Introduction

Therapeutic aerosols, which deliver active pharmaceutical ingredients to the lung, are used extensively in the treatment of respiratory diseases. Spray drying is considered a suitable manufacturing process for the production of microparticles (Broadhead et al., 1992). The processing conditions may have a tangible impact on the aerosol's performance by affecting the physical properties of the microparticles that compose it (Dobry et al., 2009). The product properties of the respiratory therapeutics, such as emitted dose or fine particle fraction, are strongly affected by physical properties of these microparticles, e.g., surface energy, roughness or stiffness (Weiler et al., 2010). As the pharmaceutical industry continues to implement more sophisticated therapeutic aerosol technology, a detailed comprehension of formulation and process variables and their influence on product performance is becoming increasingly necessary. Several inherent characteristics of an aerosol, e.g., stabilization of the active drug, powder dispersibility, and transport and deposition into the lung, are under the direct control of its microparticles' properties (Lechuga-Ballesteros et al., 2008). These particle properties must be thoroughly understood and controlled to allow for the rational design of desired aerosol properties.

There is also a need to introduce practical means to counter the ever increasing cost of drug development, e.g., affected by high cost of the active pharmaceutical ingredient or time consuming empirical formulation studies. We propose the use of mechanistic process models (Dobry et al., 2009; Ivey and Vehring, 2010) and application of existing particle engineering theory (Vehring, 2008) to achieve a more efficient, streamlined development process. Further cost savings can be achieved by selecting or implementing analytical techniques for key particle properties that require relatively small sample masses.

We demonstrate the feasibility of this approach with a formulation study that was undertaken to define a vehicle system for respiratory delivery of a biological pharmaceutical active. The two excipients used for this purpose are α,α-trehalose and L-leucine. Trehalose is often used as an excipient because of its ability to stabilize biological active pharmaceutical ingredients and to increase their shelf life (Ameri and Maa, 2006; Sastry and Agmon, 1997; Satpathy et al., 2004). L-leucine is another excipient that has gained attention in the pharmaceutical industry due to its ability to increase dispersibility and bioavailability of therapeutic aerosols (Ganderton et al., 2006; Staniforth, 2002; Vehring et al., 2011). Its use for this purpose is well documented (Batycky et al.,

* Corresponding author. Tel.: +1 780 492 5180; fax: +1 780 492 2200.
E-mail address: reinhard.vehring@ualberta.ca (R. Vehring).

0378-5173/$ – see front matter © 2011 Elsevier B.V. All rights reserved.
doi:10.1016/j.ijpharm.2011.02.049

2003; Garcia-Contreras et al., 2007; Learoyd et al., 2009; Li and Birchall, 2006; Li et al., 2005; Sung et al., 2009; Wong et al., 2007). However, despite its widespread use in development and research studies, there remains uncertainty about the formation mechanism of L-leucine microparticles and why L-leucine is so effective at enhancing dispersibility.

The most likely reason for L-leucine's ability to enhance dispersibility is its ability to form hollow particles resulting in low particle density (Lucas et al., 1999). It has been shown that a change in particle morphology, from solid spheres to hollow, rugose particles, can have a large effect on an aerosol's density and, ultimately, its dispersibility (Lechuga-Ballesteros et al., 2008). It has been suggested that the surface activity of L-leucine causes the formation of a leucine surface layer that interferes with the diffusion of water vapor, whereby hollow particles may be formed (Lähde et al., 2008; Raula et al., 2010; Wang et al., 2009). Because this theory does not fully explain the observation that a di-peptide with similar properties to leucine, but without surface activity, also produces low density particles on drying (Vehring et al., 2007), a different particle formation mechanism (Vehring, 2008) is employed to design the present study: in brief, leucine is expected to crystallize during drying, due to its low solubility, and the crystals are then expected to accumulate on the receding droplet surface because of their low mobility (Vehring et al., 2007). Hence, it is expected that the crystallinity of leucine is a key parameter that determines the details of leucine particle formation during droplet evaporation. The present study focuses on the effect that leucine crystallinity has on the morphology and the corresponding density and dispersibility of spray dried trehalose and L-leucine microparticles.

2. Theory

The solid-state physical properties and morphology of manufactured aerosol microparticles are governed by various interacting physical and chemical mechanisms during their formation. Two main factors are material properties of the formulation components and manufacturing process parameters. In general, the evaporation and particle formation kinetics for microdroplets in a spray dryer need to be described via numerical models (Vehring et al., 2007), because they are governed by coupled heat and mass transfer processes. However, a simpler analytical description (Vehring, 2008) is used here, which is valid for cases where the evaporation rate can be approximated to be constant for most of the drying process. The evaporation rate, κ, ultimately controls the evaporation of spray dried droplets and is directly related to the drying gas temperature and relative humidity, which are manufacturing process parameters. Because it determines the recession velocity of the droplet surface, the evaporation rate represents one of two main counteracting mechanisms that govern the radial concentration profiles of different excipients in the evaporating droplets. The second mechanism, described by the diffusion coefficient, D, controls how fast the excipients can redistribute inside the shrinking droplet. The effect of these two mechanisms can be summarized by the non-dimensional Peclet number, Pe (Leong, 1987) of each component:

$$Pe_i = \frac{\kappa}{8D_i} \tag{1}$$

The Peclet number can be used to describe the radial distribution of excipients in the drying droplet. A Peclet number close to 1 indicates a shallow concentration gradient with a surface enrichment of about 1.2, whereas a large Peclet number corresponds to a steep concentration gradient with large surface enrichment. Leucine and trehalose both have Peclet numbers near one for the drying conditions chosen in this study. As shown in Fig. 1, both excipients show a similar radial distribution with low surface enrichment.

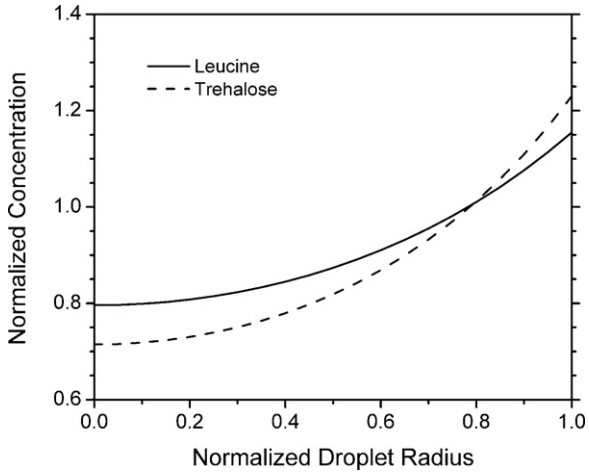

Fig. 1. Radial distribution of the excipients leucine and trehalose in an evaporating droplet with a constant evaporation rate of 4.35 μm^2/ms. The concentrations are normalized by the mean concentration and the radial position is normalized by the droplet radius.

The surface enrichment, E, for excipient i, is defined as the ratio of the surface concentration, c_s, to the mean droplet concentration, c_m. It can be approximated with good accuracy for Peclet numbers smaller than 20 by the expression (Vehring et al., 2007):

$$E_i = \frac{c_{s,i}}{c_{m,i}} = 1 + \frac{Pe_i}{5} + \frac{Pe_i^2}{100} - \frac{Pe_i^3}{4000} \tag{2}$$

At the final stage of the drying process, as the dry particle starts to form, it is expected that the morphology of the resulting particle is then determined, in part, by its surface composition as predicted by Eq. (2). Given the small surface enrichment shown in Fig. 1, the theory predicts that all droplets spray dried with the evaporation rate chosen in this study should form fairly homogeneous solid particles, regardless of their excipient concentrations.

However, various studies have demonstrated that spray dried L-leucine microparticles become hollow with thin shells as L-leucine concentration increases (Lucas et al., 1999; Najafabadi et al., 2004), in spite of its relatively low Peclet number. Thus a second mechanism that is not described by simple diffusion must be causing additional surface enrichment of leucine. One possible mechanism is the crystallization of the L-leucine component.

Because of its low solubility in water (Tseng et al., 2009), leucine is the first excipient to reach saturation at the surface, which may initiate crystallization. The constant evaporation rate model allows the definition of characteristic times to describe the kinetics of this process. The droplet drying time, i.e., the time it takes for the droplet to reach a diameter of zero, follows from the initial droplet diameter, d_0 (Vehring, 2008):

$$\tau_D = \frac{d_0^2}{\kappa} \tag{3}$$

The time it takes for each excipient to reach saturation at the surface can be calculated (Vehring, 2008) using the initial concentration of excipient i, $c_{0,i}$, in combination with its solubility, $c_{sol,i}$:

$$\tau_{sat,i} = \tau_D \left(1 - \left(\frac{c_{0,i}E_i}{c_{sol,i}}\right)^{2/3}\right) \tag{4}$$

The example shown in Fig. 7 displays the characteristic times for the conditions selected in this study. The difference between the droplet drying time and the time to reach saturation at the surface is the time available for crystallization. This time is called the precipitation time, τ_P, and it increases with the concentration of leucine to

Table 1
Parameters characterizing formulation, particle formation, and particle and powder properties.

Mass fraction of L-leucine in formulation	0	5	10	15	20	25	30	40	100[a]
Total feed concentration, in mg/mL	20.5	21.7	23.3	24.6	26.1	28.9	31.4	34.8	2
Time to reach leucine saturation, in ms	NA	9.7	8.7	7.8	6.9	5.8	4.7	2.7	73
Time available for crystallization, in ms	NA	1.6	2.6	3.5	4.4	5.5	6.6	8.6	19
Interfering trehalose concentration, in mg/mL	NA	491	232	146	103	77	60	39	0
Average C.B. density at 35.3 kPa, in kg/m^3	544	749	853	841	738	401	449	345	137
Approximate particle density, in kg/m^3	730[b]	1000[b]	1140	1120	980	540	600	460	180
Approximate MMAD of primary particles, in μm	(1.8)	(2.0)	2.0	2.1	2.1	1.9	2.0	2.0	1.9
MMAD ratio, aerosol/primary particles	(2.3)	–	2.7	2.2	1.9	2.1	1.5	1.3	1.1

[a] Spray dried using a mesh plate with larger orifice diameter.
[b] Close packing likely not achieved.

the power of two thirds (Vehring, 2008). Values for the precipitation time of leucine for the processing and formulation conditions in this study are given in Table 1. Trehalose reaches surface saturation very late; the remaining precipitation time is not sufficient for crystallization, hence, trehalose remains amorphous. An increase in L-leucine mass fraction makes leucine more likely to crystallize because it reaches saturation earlier, whereas the surface concentration of trehalose is still low. This may result in less interference from trehalose during the nucleation and crystallization of leucine.

After leucine begins to crystallize, the Peclet number for dissolved leucine is no longer applicable. The newly formed crystals have a much larger size than the leucine molecules, which reduces their diffusion coefficient by orders of magnitude. The Peclet number for leucine crystallites is now very large and rapid surface accumulation can be expected, regardless of where the crystallization is initiated. This hypothesis was the basis of the experimental design for the present study. The shell formation of leucine may be aided by its surface activity, but the proposed mechanism also provides an explanation for shell formation with excipients that are not surface active.

3. Materials and methods

3.1. Materials

L-leucine (CAS 61-90-5, Sigma Aldrich Cat# L8000) and α,α-trehalose (CAS 6138-23-4, Fisher Bioreagents Cat# BP2687) are the two excipients that were used in this experiment. To avoid contamination of the particle with foreign matter, deionized ultrafiltered water (Fisher Scientific Cat# W2-20) was used to dissolve the excipients.

3.2. Experimental design

The microparticles designed in this study are intended for respiratory delivery of potentially heat sensitive biological pharmaceutical ingredients to the lung. Hence, the following process and particle targets were set: outlet temperature, 45 °C; outlet RH, <10%, aerodynamic diameter of the primary particles, 2 μm. The feed stock flow rate for the vibrating mesh atomizer used in this experiment was chosen based on the operating conditions that produced the most stable spray. The other spray drying process variables were calculated using the methodology presented in (Ivey and Vehring, 2010).

All manufactured particles were targeted to have a similar aerodynamic diameter to allow direct comparison of powder dispersibility based on the mass median aerodynamic diameter of their aerosols. Consequentially, the feed concentration, c_F, was not kept constant in the experimental design. The aerodynamic diameter, d_a, can be calculated using the definition of the aerodynamic diameter in combination with a mass balance (Vehring, 2008). It follows that

$$d_a = \sqrt[6]{\frac{\rho_P}{\rho^*}}\sqrt[3]{\frac{c_F}{\rho^*}}d_o \quad (5)$$

where d_0 denotes the diameter of the atomized droplets and ρ^* is unit density. The particle density, ρ_P, was expected to be a strong function of composition. It was estimated beforehand as a function of leucine mass fraction, based on various published electron micrographs of leucine containing particles (Ibrahim et al., 2010; Raula et al., 2007). With this estimate, the feed stock concentrations, listed in Table 1, were chosen according to Eq. (5), such that particles with a target aerodynamic diameter of 2 μm were produced, irrespective of composition.

According to the proposed particle formation hypothesis for leucine particles, a key parameter determining the morphology of the particles is the time available for crystallization. Because the evaporation rate and initial droplet diameter were fixed, the only remaining free variable affecting this characteristic time was the initial concentration of leucine in the droplets. The total feed concentration was already determined by the targeted aerodynamic diameter. Hence, the experiment was conducted by varying the mass fraction of leucine in two-component formulations of leucine and trehalose. The mass fractions were chosen to provide approximately even spacing in the time available for crystallization, as listed in Table 1.

3.3. Methods

The crystallinity, morphology, and density of spray dried microparticles composed of trehalose and L-leucine were characterized as a function of the formulation's leucine mass fraction. Raman spectroscopy, scanning electron microscopy and a novel compressed bulk density measurement method were used to determine microparticle morphology, crystallinity and density, respectively. The mass median aerodynamic diameter (MMAD) and geometric standard deviation (GSD) of aerosols produced from the spray dried powders were also measured using a time-of-flight based method.

3.4. Spray drying

In this experiment, a Büchi B-90 Nano Spray Dryer (Büchi Labortechnik AG, Flawil, Switzerland), housed in an environmentally controlled enclosure, was used to produce powders. The B-90 spray dryer uses a unique atomizer and collector combination: a piezoelectric-driven ultrasonic atomizer, and an electrostatic collector. One advantage of the B-90 Nano Spray Dryer relative to traditional cyclone collection is that the electrostatic precipitator collects even thin walled particles without breaking them. The collector also provides good yields for small batch sizes.

In the present work, the drying gas temperature was held constant at 75 °C to produce an initial evaporation rate of

approximately 4.4 μm²/ms. The resulting droplet drying time was calculated to be 11.3 ms, based on an initial droplet diameter of 7 μm for the Büchi B-90 Nano Spray Dryer's 4.0 μm vibrating mesh plate (Li et al., 2010; Schmid et al., 2010). Droplets were dried in air with a flow rate of 100 L/min.

3.5. Electron microscopy

Particle images were taken using a JEOL 6301F scanning electron microscope (SEM) to investigate particle surface morphology. Samples were prepared on aluminum pin stubs using double sided carbon tape and sputter coated with Au (Xenosput XE200). An accelerating voltage of 5.0 kV was used at magnifications varying from 1000 to 5000×. All images were taken using secondary electron imaging.

3.6. Raman spectroscopy

The solid state of the spray dried trehalose leucine formulations was analyzed using dispersive Raman spectroscopy. The custom Raman system and the methodology used to determine the crystalline and amorphous components of the powders are described in detail elsewhere (Vehring, 2005). Briefly, Raman spectra were excited with a diode laser operating at a wavelength of 670 nm. Raman scattering was analyzed using a single stage Czerny–Turner spectrograph with an additional filter stage, and a cooled CCD sensor as detector. The volume of the sample holder in this instrument was 1.1 μL. Consequently, the required sample mass for Raman analysis was less than 1.5 mg. Because such small powder quantities are expected to rapidly take up water when exposed to standard laboratory conditions (Gil et al., 1996; Umprayn and Mendes, 1987), measures were taken to avoid exposure of the powder samples to humid environments: the powders were sampled in a dry atmosphere enclosure and transferred to the Raman system in a sealed transfer container. In the Raman system the samples were placed and analyzed on a temperature controlled base in a closed sample chamber under nitrogen atmosphere. All spectra were taken at a temperature of 21 ± 1 °C and a relative humidity of less than 5%.

Fig. 2 shows the reference spectra used in the spectral deconvolution of the powder spectra.

The top spectrum, labeled Tre,dh, was measured from the trehalose raw material used in the study. As expected, it is representative of the crystalline dihydrate form of trehalose ($C_{12}H_{22}O_{11}\cdot 2H_2O$) (Gil et al., 1996). No crystalline trehalose was detected in the powder samples. The Raman spectrum measured from pure spray dried trehalose is shown in the second trace from the top in Fig. 2, labeled Tre,am. The spectrum is that of amorphous trehalose (Chakravarty et al., 2009). Because trehalose was found to be amorphous in all spray dried formulations, its known mass fraction, Y_{Tre}, was selected as the internal standard for quantitative analysis of the leucine components. Hence, the mass fractions, $Y_{Leu,i}$, of amorphous and crystalline leucine were calculated using the relationship (Vehring, 2005):

$$Y_{Leu,i} = Y_{Tre} k_{Leu,i,Tre} \frac{a_{Leu,i}}{a_{Tre}} \quad (6)$$

The calibration factors $k_{Leu,i,Tre}$ were derived from a formulation that had no detectable amorphous leucine ($Y_{Tre} = 0.6$, $Y_{Leu,c} = 0.4$) in combination with the condition $\sum Y_i = 1$.

The intensity factors, a, were obtained from deconvolution of the sample spectra, S, into the three normalized reference spectra, S_i, shown in Fig. 2, specifically $S_{Tre,am}$, $S_{Leu,c}$, and $S_{Leu,am}$, according to

$$S = B + \sum_i a_i S_i(\Delta\nu + b_i) \quad (7)$$

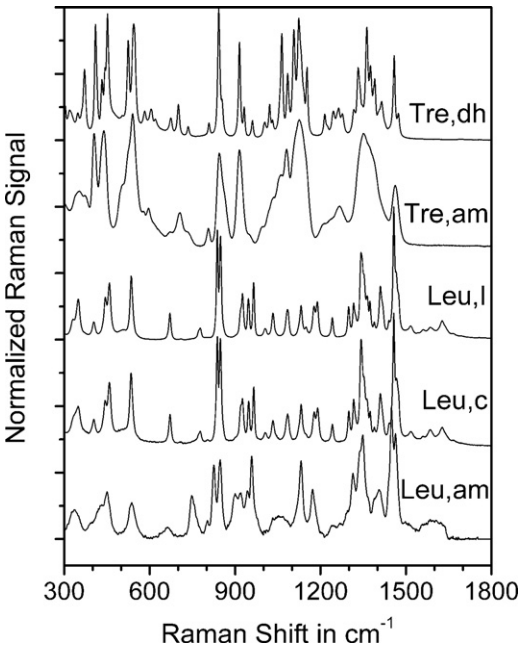

Fig. 2. Reference spectra used for the Raman measurements. From top to bottom: raw material, crystalline trehalose dihydrate; spray dried amorphous trehalose; raw material, crystalline L-leucine, polymorph I; principal component for crystalline leucine in spray dried powders; principal component for amorphous leucine in spray dried powders.

where b_i denotes a wavenumber shift correction that accounts for small changes in the laser excitation wavelength between measurements. B is a low order polynomial used to subtract the measurement background. Using the three normalized reference spectra more than 98% of the signal in all measurements could be deconvoluted. The spectrum labeled Leu,c was very similar but not identical to the Raman spectrum of the Leucine raw material, Leu,l, identified as the polymorph I of L-leucine (Bougeard, 1983), the expected form at standard conditions (Moggach et al., 2008). The observed minor differences in the spectra were minimal when the spectrum of raw material at an elevated temperature of 55 °C was used for comparison, a temperature that is still below the transition temperature to polymorph II at 80 °C (Grunenberg et al., 1984). This may indicate that the leucine microcrystals in the spray dried powders have a slightly altered unit cell geometry compared to macroscopic crystals. The spectrum labeled Leu,am was similar to a spectrum of a saturated leucine solution. Because the Raman spectra of amorphous solids typically resemble that of their concentrated solution (Söderholm et al., 1999; Vehring, 2005) this spectrum was used as a representation of the amorphous leucine fraction.

3.7. Powder density

Tap density measurements require a significant amount of aerosol powder, typically in the range of several grams (PhEur, 2010; USP, 2010), and its applicability to powders in the respirable size range appears questionable due to the relatively low importance of inertial forces for such small particles. In response to the limitations of common tap density measurements, a more adequate method of measuring powder density that uses only milligrams of powder was developed. The instrument measures the density of a powder volume under defined pressure, similar to a commercially available instrument for larger sample masses (Micromeritics Geopyc 1360).

A cylindrical cavity was loosely filled with a known mass of powder and then placed on an analytical balance. A mating micrometer head spindle (Mitutoyo Micrometer Head Series 153-Non-Rotating Spindle Type) was used as a piston to compact the powder sample. The micrometer head was vertically aligned with the cavity using a custom clamping mechanism and vertical support structure. By zeroing the micrometer head with the top of the cylindrical cavity, the amount of force applied by the micrometer piston was accurately measured as a function of the powder bed's volume change. From these values, a correlation between density and the applied pressure was obtained. Literature has demonstrated that for a similar method a pressure of 35.3 kPa yields equivalent density values to those obtained from tap density measurements (Thalberg et al., 2004). To ensure this pressure gives an accurate representation of the compressed bulk density (CBD), SEM micrographs (not shown) of the powder bed were taken before and after compression at 35.3 kPa. No indication of fractured particles was found. The compressed bulk density was also reported at a pressure of 5 kPa to study differences in the compressibility of the powder bed.

3.8. Particle size and dispersibility

The mass median aerodynamic diameter (MMAD) and geometric standard deviation (GSD) of the spray dried materials were determined with an Aerodynamic Particle Sizer (APS, TSI Model 3321). Aerosols of the spray dried materials were generated with dry powder insufflators (Penn Century) into the APS, without a diluter, via a 3 mL syringe.

4. Results

4.1. Crystallinity

The results of the deconvolution of the Raman spectra, as described in Section 3.6, are shown in Fig. 3. A distinct transition in leucine crystallinity was observed with increasing leucine mass fraction in the formulation. The trehalose component remained amorphous across all formulations. For formulations with a leucine mass fraction larger than 25% no amorphous leucine was detected. This includes the pure leucine formulation, which is not shown in the graph.

The formulation with 5% leucine content showed a dominant amorphous signal, but the result was not included in the graph, because the small absolute amount of leucine in this formulation approached the limit of quantification.

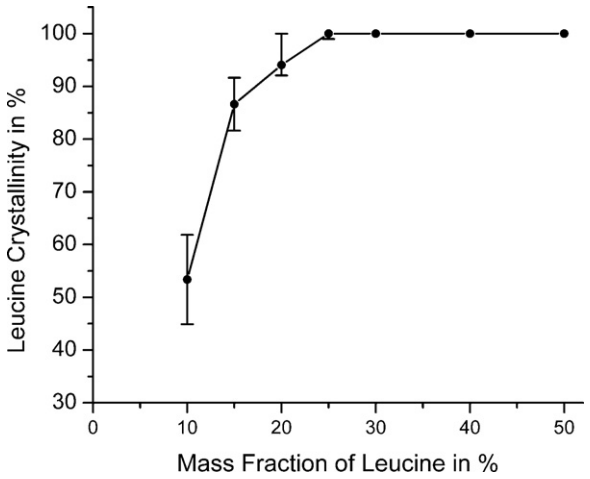

Fig. 3. Crystallinity of leucine as a function of leucine content in powders that were spray dried under identical process conditions.

4.2. Morphology

As depicted in Fig. 4, the morphology of the spray dried microparticles changed, as expected, from solid, smooth spheres to hollow particles with thin shells for increasing L-leucine mass fraction. All pictures in Fig. 4 were taken with a magnification of 5000×. Each panel shows a typical field of view of 25 μm × 20 μm for the indicated formulation.

As the mass fraction of leucine increased, the fraction of hollow, thin walled particles increased, becoming the most prevalent morphology type for leucine mass fractions ≥25%. The powder with 10% leucine mass fraction had a similar appearance to the smooth spheres of the pure trehalose formulation. The surface of the particles became more corrugated as the leucine mass fraction increased. This effect was visible even on apparently solid, spherical particles at 10% and 15% leucine mass fraction. An increase in median geometric particle diameter with increasing leucine mass fraction was clearly visible, indicating a significant reduction in particle density.

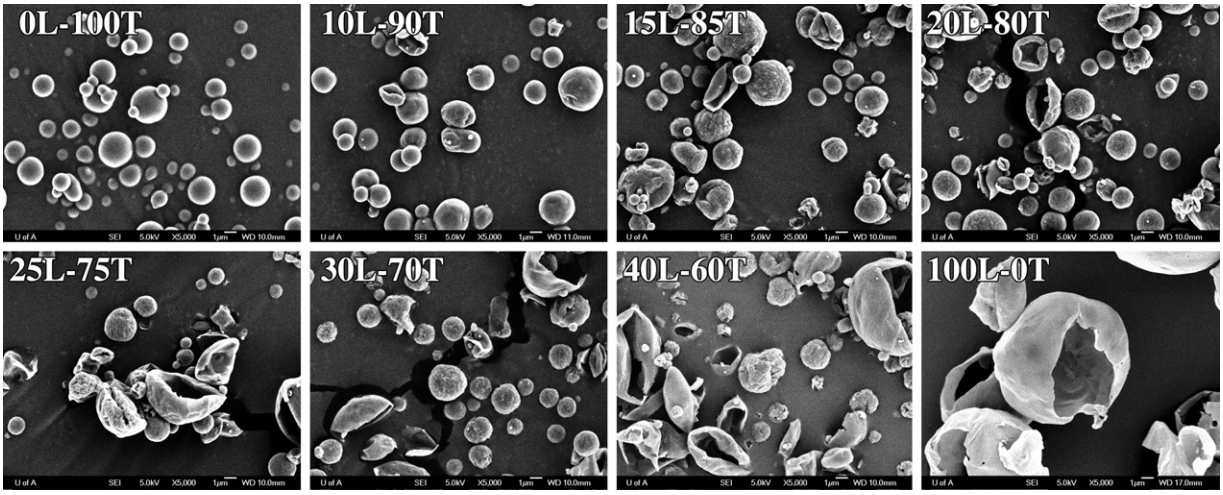

Fig. 4. Morphology of spray dried leucine (L) – trehalose (T) microparticles with varying mass fractions of leucine as indicated in the panel labels. The median aerodynamic particle diameter of the particles was about 2 μm in all formulations. All pictures were taken at a magnification of 5000×. Each panel has a field of view of 25 μm × 20 μm.

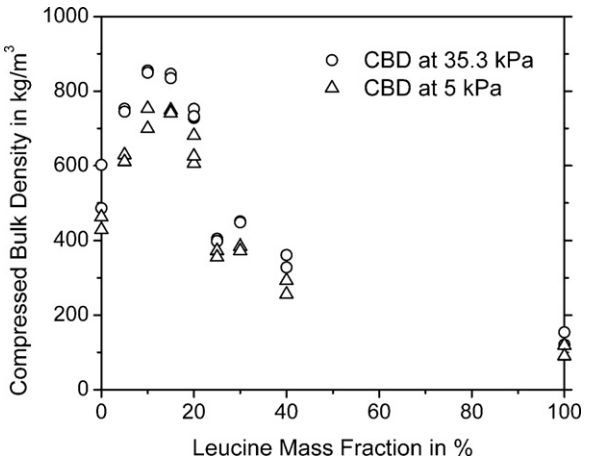

Fig. 5. Powder density measured at defined pressures on the powder bed. The open circles represent a pressure of 35.3 kPa roughly equivalent to a tap density measurement.

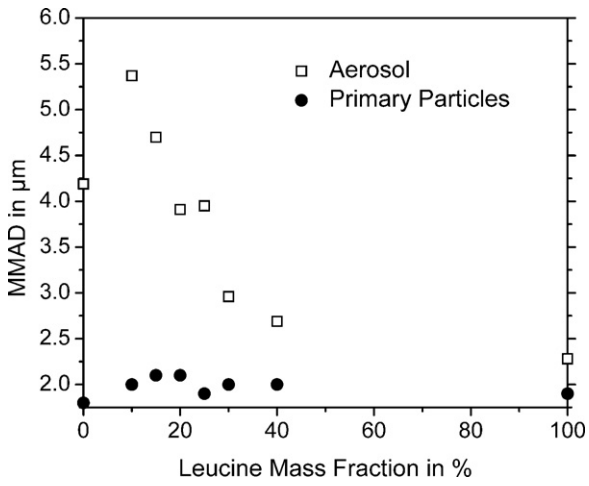

Fig. 6. Mass median aerodynamic diameter of primary particles (approximate) and of the respective aerosol dispersed with a Penn Century powder disperser.

4.3. Powder density

Fig. 5 illustrates the change in compressed bulk density (CBD) at pressures of 35.3 and 5 kPa as a function of leucine mass fraction. The highest powder density was observed for formulations with a 10% L-leucine mass fraction. A significant decrease in average CBD was observed between L-leucine mass fractions of 20% and 25%, respectively. This large change in density corresponded to the observed transitions in leucine crystallinity and the change in particle morphology. Powder density values taken at a pressure of 5 kPa mirrored the trend observed at 35.3 kPa. Similar to the measurements obtained at 35.3 kPa, the average CBD value of 20% leucine at 5 kPa was almost halved as the leucine mass fraction increased from 20% to 25%. The compressed bulk density of trehalose and the morphologically similar formulation with 5% leucine mass fraction were lower than that of the 10% leucine formulation and significantly lower than the density expected for a closely packed powder of solid trehalose spheres. It has been shown before that pure trehalose forms solid particles under similar drying conditions (Vehring et al., 2007). However, it was noted during the density measurements that the formulations without leucine or low leucine content were very cohesive, making compaction of the powders difficult. Pure trehalose powder strongly adhered to the micrometer piston head and cavity. This effect caused large fluctuations in the observed CBD and made it unlikely that close packing of the particles was achieved.

4.4. Aerodynamic diameter

Fig. 6 depicts the MMAD values for the aerosols that were generated from all formulations using a simple disperser. MMAD values ranged between 2.13 μm and 5.37 μm, decreasing with increasing L-leucine mass fraction in a pattern similar to that of the powder density measurements, within experimental error. A minimum leucine mass fraction of 15% was necessary for particles to disperse with an MMAD in the commonly accepted range for respirable particles (1–5 μm) (Patton and Byron, 2007; Shekunov et al., 2007). It should be noted that the MMAD from the insufflator is useful for rank ordering different formulations according to their dispersibility, but not equivalent to the aerosol performance of a dry powder inhaler in patient use.

Also shown in Fig. 6 is an approximate value for the MMAD of the primary particles of the spray dried powders. This value was calculated using Eq. (5). As a surrogate for the unknown particle density, we used the compressed bulk density at 35.3 kPa divided by an estimated packing factor of 0.74, valid for close packing of spheres. Because the aerodynamic diameter as described by Eq. (5) is a weak function of the particle density, a rough approximation is sufficient. The estimated particle density and the resulting MMAD of the primary particles are listed in Table 1. The result demonstrates that the initial estimate for the particle density in the experimental design was close enough to achieve particles with a primary aerodynamic particle size near 2 μm for all formulations. The discrepancy between the aerodynamic particle size of the primary particles and that of the aerosol can be explained by incomplete dispersion of the powder.

5. Discussion

The morphology of aerosol microparticles composed of leucine changed from solid spheres with corrugated surfaces to hollow particles as the leucine mass fraction increased. The correlation of this morphological change with the particle's change in crystallinity suggests that the mechanism for the formation of the observed thin shells is the crystallization of leucine. The change in crystallinity also correlates well with the decrease in compressed bulk density – a direct result of the formation of hollow particles. These findings suggest that leucine crystallinity may be used as an indicator for particle morphology and aerosol dispersibility in formulation studies involving leucine.

Crystallinity, powder density, and MMAD of the aerosol show a non-linear response to a change in leucine mass fraction, with each of these properties undergoing a distinct transition at a leucine mass fraction of 25%. This was the point at which the microparticles' leucine component became completely crystalline, formed predominantly hollow shells as opposed to solid spheres, and experienced a significant drop in powder density. The mass fraction of leucine necessary to initiate these changes may be affected by a third component in the formulation, e.g., a pharmaceutical active. However, the results indicate that a minimum amount of leucine must be exceeded to achieve the commonly known beneficial effects on dispersibility.

As described previously, particle formation theory predicts that an increase in leucine mass fraction results in an earlier onset of crystallization, explaining the increase in its crystalline character. Table 1 shows the times to reach saturation, the times available for crystallization for leucine, and the corresponding trehalose surface concentration at the time when leucine reaches saturation, all calculated as functions of leucine mass fraction. The surface concentration of the trehalose component, which may interfere with

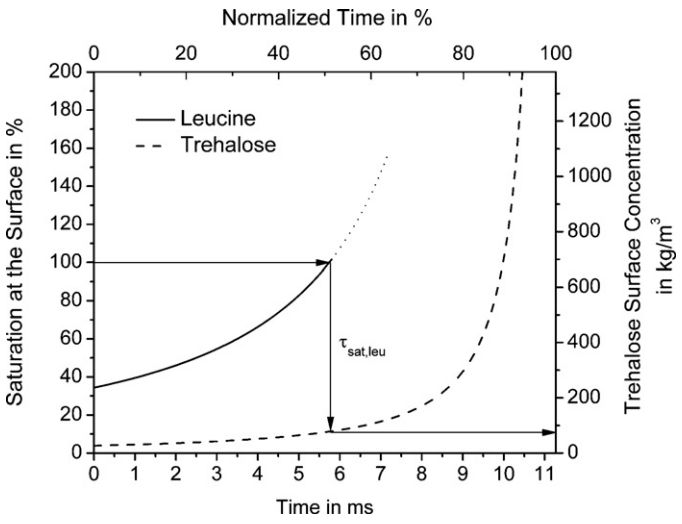

Fig. 7. Predicted surface concentration of L-leucine and trehalose during evaporation of a formulation with 25% leucine mass fraction. Bottom and right (for trehalose) axis are absolute. The left axis is normalized by the solubility of the excipients; the top axis is normalized by the droplet drying time.

leucine nucleation or crystallization, decreases as the leucine mass fraction is increased. Trehalose's surface concentration is calculated at a point in time where leucine reaches surface saturation, as shown in Fig. 7. With more time to crystallize and less interference from trehalose, the leucine component of the manufactured microparticles becomes more crystalline as the leucine content increases.

The results are consistent with the proposed formation mechanism: crystallization triggers an increase in Peclet number, because the newly formed crystals have a much lower diffusion coefficient than the dissolved leucine molecules. The greater Peclet number corresponds to a significant increase in the droplet surface enrichment, thus causing the formation of a shell.

An important consequence of leucine's crystallization and the resultant formation of hollow particles is its effect on powder density and dispersibility. Compressed bulk density values responded to the formation of hollow particles by decreasing appreciably. As leucine achieved complete crystallinity at a mass fraction of 25%, the aerosol powder bed experienced a 43–46% decrease in density. The lower density and increased particle rugosity led, as expected (Chew and Chan, 2001; Chew et al., 2005), to improved dispersibility and consequentially a smaller MMAD. Together these properties are expected to yield an increase in the aerosol's respirable fraction and ability to reach the deep lung (Leach et al., 2009). A useful measure for the dispersibility of the manufactured powders is the ratio of the MMAD of the aerosol to that of the primary particles, listed in Table 1. While specific to the method of dispersion, it allows a fair comparison between the particles in this study, because all primary particles were manufactured with about the same aerodynamic diameter. The results, shown in Table 1, clearly show that adding a small amount of leucine, which results in only partial crystallization and insignificant change in morphology from a solid sphere, does not provide improved dispersibility relative to the pure trehalose powder. Powders with high trehalose content dispersed very poorly from the Penn-Century insufflator. The resulting particle size distributions for these formulations were, in some instances, bimodal. It is known that trehalose and other similar sugar excipients are very cohesive under atmospheric conditions, causing the agglomeration of aerosol particles (Gianfrancesco et al., 2009). The multi-modal distributions were most likely due to severe agglomeration of trehalose particles, because a thorough review of electron micrographs did not reveal a large particle mode in the primary particles.

6. Conclusions

A systematic, mechanistic approach to microparticle design in pharmaceutical applications becomes increasingly important as advancements in therapeutic aerosols call for increased particle complexity. Furthermore, a thorough understanding of the solid-state properties of microparticles and how they affect powder and aerosol behavior is necessary. The present work demonstrates, in particular, the inter-relation between initial leucine mass fraction and the kinetics of particle formation with the resulting particle morphology, crystallinity and powder density of spray-dried microparticles composed of trehalose and L-leucine. It was found that crystalline leucine was necessary to obtain low-density, well dispersing particles. A minimum leucine threshold must be exceeded to obtain these advantages. The observed results lend support to the proposed particle formation mechanism for leucine containing particles. This hypothesis can provide a mechanistic understanding that can be employed for efficient experimental design of future formulation studies. A more targeted approach to designing and characterizing microparticles can be created. Based on several known initial conditions and targets (droplet size, drying temperature, initial excipient concentration, saturation concentration), it is possible to calculate the remaining processing conditions and characteristic times for particle formation. By targeting specific L-leucine mass fractions that yield sufficient crystalline character, it is possible to quickly attain desirable qualities of aerosol solid-state properties such as morphology, CBD and dispersibility. This would eliminate the need for extensive and time-consuming empirical formulation studies.

Furthering the efficiency of this approach is the minimal amount of powder manufactured and used throughout the process. Crystallinity, morphology, powder density, and aerosol particle size were all assessed using less than 80 mg of powder. Raman spectroscopy successfully analyzed the amorphous and crystalline leucine and trehalose components on less than 5 mg of powder. The novel CBD measurement technique introduced here requires less than 30 mg of powder per measurement. Small batch sizes allow for the economical use of expensive active pharmaceutical ingredients, which is ideal for research and early development applications. The mechanistic models and analytical techniques used in this study introduce a more efficient and time- and cost-effective formulation strategy for particulate dosage forms.

References

Ameri, M., Maa, Y.-F., 2006. Spray drying of biopharmaceuticals: stability and process considerations. Drying Technol. 24, 763–768.
Batycky, R.P., Lipp, M.M., Niven, R.W., 2003, Use of simple amino acids to form porous particles during spray drying, USA Patent # 6,586,008.
Bougeard, D., 1983. Phase transition and vibrational spectra of L-leucine. Ber. Bunsen-Ges. Phys. Chem. 87, 279–283.
Broadhead, J., Edmond Rouan, S.K., Rhodes, C.T., 1992. The spray drying of pharmaceuticals. Drug Dev. Ind. Pharm. 18, 1169–1206.
Chakravarty, P., Bhardwaj, S.P., King, L., Suryanarayanan, R., 2009. Monitoring phase transformation in intact tablets of trehalose by FT-Raman spectroscopy. AAPS Pharm. Sci. Technol. 10, 1420–1426.
Chew, N.Y.K., Chan, H.-K., 2001. Use of solid corrugated particles to enhance powder performance. Pharm. Res. 18, 1570–1577.
Chew, N.Y.K., Tang, P., Chan, H.-K., Raper, J.A., 2005. How much particle surface corrugation is sufficient to improve aerosol performance of powders? Pharm. Res. 22, 148–152.
Dobry, D., Settell, D., Baumann, J., Ray, R., Graham, L., Beyerinck, R., 2009. A model-based methodology for spray-drying process development. J. Pharm. Innovation 4, 133–142.
Ganderton, D., Morton, D.A.V., Lucas, P., 2006, Powders, USA Patent # 6,989, 155.
Garcia-Contreras, L., Fiegel, J., Telko, M.J., Elbert, K., Hawi, A., Thomas, M., VerBerkmoes, J., Germishuizen, W.A., Fourie, P.B., Hickey, A.J., Edwards, D., 2007. Inhaled

large porous particles of capreomycin for treatment of tuberculosis in a Guinea pig model. Antimicrob. Agents Chemother. 51, 2830–2836.
Gianfrancesco, A., Turchiuli, C., Dumoulin, E., Palzer, S., 2009. Prediction of powder stickiness along spray drying process in relation to agglomeration. Part. Sci. Technol. 27, 415–427.
Gil, A.M., Belton, P.S., Felix, V., 1996. Spectroscopic studies of solid [alpha]-[alpha] trehalose. Spectrochim. Acta. Part A: Mol. Biomol. Spectrosc. 52, 1649–1659.
Grunenberg, A., Bougeard, D., Schrader, B., 1984. DSC-Investigation of 22 crystalline neutral aliphatic amino acids in the temperature range 233–423 K. Thermochim. Acta 77, 59–66.
Ibrahim, B., Jun, S., Lee, M., Kang, S., Yeo, Y., 2010. Development of inhalable dry powder formulation of basic fibroblast growth factor. Int. J. Pharm. 385, 66–72.
Ivey, J., Vehring, R., 2010. The use of modeling in spray drying of emulsions and suspensions accelerates formulation and process development. Comput. Chem. Eng. 34, 1030–1035.
Lähde, A., Raula, J., Kauppinen, E., 2008. Simultaneous synthesis and coating of salbutamol sulphate nanoparticles with L-leucine in the gas phase. Int. J. Pharm. 358, 256–262.
Leach, C., Colice, G., Luskin, A., 2009. Particle size of inhaled corticosteroids: does it matter? J. Allergy Clin. Immunol. 124, S88–S93.
Learoyd, T., Burrows, J., French, E., Seville, P., 2009. Sustained delivery by leucine-modified chitosan spray-dried respirable powders. Int. J. Pharm. 372, 97–104.
Lechuga-Ballesteros, D., Charan, C., Stults, C., Stevenson, C.L., Miller, D.P., Vehring, R., Tep, V., Kuo, M.-C., 2008. Trileucine improves dispersibility, aerosol performance and stability of spray-dried powders for inhalation. J. Pharm. Sci. 97, 287–302.
Leong, K.H., 1987. Morphological control of particles generated from the evaporation of solution droplets: theoretical considerations. J. Aerosol Sci. 18, 511–524.
Li, H.-Y., Birchall, J., 2006. Chitosan-modified dry powder formulations for pulmonary gene delivery. Pharm. Res. 23, 941–950.
Li, H.-Y., Seville, P.C., Williamson, I.J., Birchall, J.C., 2005. The use of amino acids to enhance the aerosolisation of spray-dried powders for pulmonary gene therapy. J. Gene Med. 7, 343–353.
Li, X., Anton, N., Arpagaus, C., Belleteix, F., Vandamme, T., 2010. Nanoparticles by spray drying using innovative new technology: the Büchi nano spray dryer b-90. J. Controlled Release 147, 304–310.
Lucas, P., Anderson, K., Potter, U.J., Staniforth, J.N., 1999. Enhancement of small particle size dry powder aerosol formulations using an ultra low density additive. Pharm. Res. 16, 1643–1647.
Moggach, S.A., Parsons, S., Wood, P.A., 2008. High-pressure polymorphism in amino acids. Crystallogr. Rev. 14, 143–184.
Najafabadi, A.R., Gilani, K., Barghi, M., Rafiee-Tehrani, M., 2004. The effect of vehicle on physical properties and aerosolisation behaviour of disodium cromoglycate microparticles spray dried alone or with L-leucine. Int. J. Pharm. 285, 97–108.
Patton, J.S., Byron, P.R., 2007. Inhaling medicines: delivering drugs to the body through the lungs. Nat. Rev. Drug Discovery 6, 67–74.
PhEur, 2010. Bulk Density and Tapped Density of Powders, 6th ed, Supplement 6.8 to Ph.Eur.
Raula, J., Kurkela, J., Brown, D., Kauppinen, E., 2007. Study of the dispersion behaviour of L-leucine containing microparticles synthesized with an aerosol flow reactor method. Powder Technol. 177, 125–132.
Raula, J., Thielmann, F., Naderi, M., Lehto, V., Kauppinen, E., 2010. Investigations on particle surface characteristics vs. dispersion behaviour of L-leucine coated carrier-free inhalable powders. Int. J. Pharm. 385, 79–85.
Sastry, G.M., Agmon, N., 1997. Trehalose prevents myoglobin collapse and preserves its internal mobility. Biochemistry 36, 7097–7108.
Satpathy, G.R., Török, Z., Bali, R., Dwyre, D.M., Little, E., Walker, N.J., Tablin, F., Crowe, J.H., Tsvetkova, N.M., 2004. Loading red blood cells with trehalose: a step towards biostabilization. Cryobiology 49, 123–136.
Schmid, K., Arpagaus, C., Friess, W., 2010. Evaluation of the nano spray dryer B-90 for pharmaceutical applications. Pharm. Dev. Technol., doi:10.3109/10837450.2010.485320.
Shekunov, B.Y., Chattopadhyay, P., Tong, H.H.Y., Chow, A.H.L., 2007. Particle size analysis in pharmaceutics: principles. methods and applications. Pharm. Res. 24, 203–227.
Söderholm, S., Roos, Y.H., Meinander, N., Hotokka, M., 1999. Raman spectra of fructose and glucose in the amophous and crystalline states. J. Raman Spectrosc. 30, 1009–1018.
Staniforth, J.N., 2002, Powders comprising anti-adherent materials for use in dry powder inhalers, USA Patent # 6,475,523.
Sung, J.C., Padilla, D.J., Garcia-Contreras, L., VerBerkmoes, J., Durbin, D., Peloquin, C.A., Elbert, K.J., Hickey, A.J., Edwards, D.A., 2009. Formulation and pharmacokinetics of self-assembled rifampicin nanoparticle systems for pulmonary delivery. Pharm. Res. 26, 1847–1855.
Thalberg, K., Lindholm, D., Axelsson, A., 2004. Comparison of different flowability tests for powders for inhalation. Powder Technol. 146, 206–213.
Tseng, H., Lee, C., Weng, W., Shiah, I., 2009. Solubilities of amino acids in water at various pH values under 298.15 K. Fluid Phase Equilib. 285, 90–95.
Umprayn, K., Mendes, R.W., 1987. Hygroscopicity and moisture adsorption kinetics of pharmaceutical solids: a review. Drug Dev. Ind. Pharm. 13, 653–693.
USP, 2010. (616) Bulk Density and Tapped Density of Powders. United States Pharmacopeia.
Vehring, R., 2005. Red-excitation dispersive raman spectroscopy is a suitable technique for solid state analysis of respirable pharmaceutical powders. Appl. Spectrosc. 59, 286–292.
Vehring, R., 2008. Pharmaceutical particle engineering via spray drying. Pharm. Res. 25, 999–1022.
Vehring, R., Foss, W.R., Lechuga-Ballesteros, D., 2007. Particle formation in spray drying. J. Aerosol Sci. 38, 728–746.
Vehring, R., Miller, D.P., Lechuga-Ballesteros, D., 2011, Pharmaceutical formulation comprising a water-insoluble active agent, USA Patent # 7,862, 834 B2.
Wang, L., Zhang, Y., Tang, X., 2009. Characterization of a new inhalable thymopentin formulation. Int. J. Pharm. 375, 1–7.
Weiler, C., Egen, M., Trunk, M., Langguth, P., 2010. Force control and powder dispersibility of spray dried particles for inhalation. J. Pharm. Sci. 99, 303–316.
Wong, Y.-L., Sampson, S., Germishuizen, W.A., Goonesekera, S., Caponetti, G., Sadoff, J., Bloom, B.R., Edwards, D., 2007. Drying a tuberculosis vaccine without freezing. Proc. Natl. Acad. Sci. 104, 2591–2595.